A Combined Computational/Experimental Study on $LiNi_{1/3}Co_{1/3}Mn_{1/3}O_2$

B. J. Hwang,[†,‡] Y. W. Tsai,[†] D. Carlier,[‡] and G. Ceder*[,‡]

Department of Chemical Engineering, National Taiwan University of Science and Technology, Taipei, 106, Taiwan, and Department of Materials Science and Engineering and Center for Materials Science and Engineering, Massachusetts Institute of Technology, Cambridge, Massachusetts 02139-4307

Received March 24, 2003. Revised Manuscript Received June 23, 2003

A combined computational/experimental study on $LiNi_{1/3}Co_{1/3}Mn_{1/3}O_2$ is presented. Both density functional theory and experiments are used to probe the active redox pairs and changes in electronic structure of $LiNi_{1/3}Co_{1/3}Mn_{1/3}O_2$ during intercalation or deintercalation of Li. The phase stability and voltage curve of this material are also shown in this paper. Both the experimental and computational data show that $LiNi_{1/3}Co_{1/3}Mn_{1/3}O_2$ material is a high-capacity stable electrode for advanced rechargeable lithium ion batteries.

Introduction

$LiCoO_2$ is currently being used as a cathode material in commercial lithium ion batteries because of its easy synthesis and good cyclability.[1] However, this material is expensive and the practically attainable rechargeable capacity is only 50% (140 mA h/g) of the theoretical capacity (274 mA h/g). $LiNiO_2$ is considerably less expensive and has a higher initial capacity (200 mA h/g) than $LiCoO_2$.[2] However, this material is known to be more difficult to synthesize and suffers from instabilities at the top of charge. Partial substitution of Ni by other metal cations has been made to enhance the $LiNiO_2$ electrochemical performance.[3−5] In particular, the solid solution, $LiNi_{1-x}Co_xO_2$, has been suggested as an alternative to $LiNiO_2$ as it combines some of the benefits of $LiNiO_2$ (capacity) with those of $LiCoO_2$ (stability).[6,7] Substitution of Ni by lower cost metals, such as Mn, has also been investigated.[8] Results of Liu et al. indicate that Mn is effective in improving initial capacity and cycle life of lithium nickel cobalt oxide.[9] Dahn and coworkers[10] have reported a series of $LiNi_xCo_{1-2x}Mn_xO_2$ compounds ($0 \leq x \leq {}^1/_2$) synthesized by a mixed hydroxide method. These materials show a specific capacity between 110 and 130 mA h/g in the range of 3.0−4.2 V. It was found that the amount of Ni in the lithium layer increases as the concentration of Ni in $LiNi_xCo_{1-2x}Mn_xO_2$ increases. In a preliminary communication, $LiNi_{1/3}Co_{1/3}Mn_{1/3}O_2$, synthesized by a solid-state method, has been reported to have a capacity of 150 mA h/g in the voltage window of 2.5−4.2 V by Ohzuku and Makimura.[11] A capacity of 200 mA h/g in the voltage window of 2.5−4.6V has also been reported by Yabuuchi and Ohzuku.[12] Shaju et al.[13] have demonstrated that the initial capacity of $LiNi_{1/3}Co_{1/3}Mn_{1/3}O_2$ synthesized by a mixed hydroxide method is 160 mA h/g in the voltage window of 2.5−4.4 V at a C/5-rate. However, the cation mixing between lithium ions and transition metal ions, and the capacity fading of these materials remains a significant problem. Recently, the electronic structure of $LiNi_{1/3}Co_{1/3}Mn_{1/3}O_2$ has been investigated by Koyama et al.[14] using first-principles calculations in the local density approximation (LDA) considering only ferromagnetic coupling. However, antiferromagnetic spin polarization has been previously demonstrated to be crucial in manganese oxides.[15]

The purpose of this paper is to clarify the valence states in $LiNi_{1/3}Co_{1/3}Mn_{1/3}O_2$ and characterize the electronic and structural changes that occur upon delithiation. In parallel, the properties of the $LiNi_{1/3}Co_{1/3}Mn_{1/3}O_2$ materials synthesized by a sol−gel method were also investigated experimentally to compare with the computational results.

Computational

All calculations are performed in the generalized gradient approximation (GGA) to density functional theory as implemented in the Vienna Ab Initio Simulation Package (VASP).

* Corresponding author. E-mail: gceder@mit.edu.
† National Taiwan University of Science and Technology.
‡ Massachusetts Institute of Technology.

(1) Nagaura, T.; Tozawa, K. *Prog. Batteries Sol. Cells* **1990**, *9*, 20.
(2) Ohzuku, T.; Ueda, A.; Nagayama, M. *J. Electrochem. Soc.* **1993**, *140*, 1862.
(3) Delmas, C.; Saadoune, I.; Rougier, A. *J. Power Sources* **1993**, *43/44*, 595.
(4) Caurant, D.; Baffier, N.; Bianchi, V.; Gregoire, G.; Bach, S. *J. Mater. Chem.* **1996**, *6*, 1149.
(5) Ohzuku, T.; Ueda, A.; Kouguchi, M. *J. Electrochem. Soc.* **1995**, *142*, 4033.
(6) Ohzuku, T.; Ueda, A.; Nagayama, M.; Iwakoshi, Y.; Komori, H. *Electrochim. Acta* **1993**, *38*, 1159.
(7) Hwang, B. J.; Santhanam, R.; Chen, C. H. *J. Power Sources* **200**3, *114*, 244.
(8) Winter, M.; Besenhard, J. O.; Spahr, M. E.; Novak, P. *Adv. Mater.* **1998**, *10*, 725.
(9) Liu, Z.; Yu, A.; Lee, J. Y. *J. Power Sources* **1999**, *81−82*, 416.
(10) MacNeil, D. D.; Lu, Z.; Dahn, J. R. *J. Electrochem. Soc.* **2002**, *149*, A1332.
(11) Ohzuku, T.; Makimura, Y. *Chem. Lett.* **2001**, 642.
(12) Yabuuchi, N.; Ohzuku, T. Extended abstract No. 122, IMLB 11, June 23−28, Monterey, CA, 2002.
(13) Shaju, K. M.; Subba Rao, G. V.; Chowdari, B. V. R. *Electrochim. Acta* **2002**, *48*, 145.
(14) Koyama, Y.; Tanaka, I.; Adachi, H.; Makimura, Y.; Ohzuku, T. Extended abstract No. 183, IMLB 11, June 23−28, Monterey, CA, 2002.
(15) Mishra, S. K.; Ceder, G. *Phys. Rev. B.* **1999**, *59*, 6120.

10.1021/cm030299v CCC: $25.00
Published on Web 08/15/2003

Table 1. Calculated Lattice Parameters of $Li_xNi_{1/3}Co_{1/3}Mn_{1/3}O_2$

x	a, Å	c, Å	Ni−O, Å	Co−O, Å	Mn−O, Å
1[a]	2.892	14.251	(4 × 2.05, 2 × 2.07)	(4 × 1.95, 2 × 1.96)	(6 × 1.94)
$^5/_6$[b]	2.891	14.398	(2.00, 2.03, 2 × 2.05, 2.07)	(1.89, 1.93, 1.94, 3 × 1.95)	(1.91, 2 × 1.93, 2 × 1.95, 1.96)
			(1.89, 1.91, 1.99, 2 × 2.04, 2.07)	(1.91, 1.93, 2 × 1.94, 1.95, 1.98)	(1.92, 1.93, 3 × 1.94, 1.95)
$^2/_3$[a]	2.884	14.503	(2 × 1.88, 4 × 2.04)	(2 × 1.89, 4 × 1.94)	(2 × 1.90, 2 × 1.93, 2 × 1.96)
$^1/_2$[b]	2.841	14.973	(1.89, 3 × 1.91, 1.92, 1.94)	(1.89, 1.90, 1.91, 1.94, 1.95, 1.97)	(1.89, 1.91, 1.93, 1.94, 2 × 1.95)
			(2 × 1.90, 1.91, 1.93, 2 × 2.12)	(2 × 1.90, 2 × 1.92, 2 × 1.93)	(1.89, 1.91, 2 × 1.93, 1.94, 1.96)
$^1/_3$[a]	2.849	14.980	(4 × 1.91, 2 × 1.93)	(4 × 1.90, 2 × 1.93)	(2 × 1.91, 2 × 1.92, 2 × 1.93)
$^1/_6$[b]	2.853	14.962	(5 × 1.90, 1.93)	(2 × 1.88, 1.90, 2 × 1.91, 1.93)	(1.90, 2 × 1.91, 2 × 1.92, 1.95)
			(2 × 1.89, 1.90, 2 × 1.91, 1.93)	(1.88, 4 × 1.90, 1.93)	(1.90, 3 × 1.91, 2 × 1.93)
0[a]	2.863	14.693	6 × 1.90	6 × 1.89	6 × 1.91

[a] Supercell with 3 formula units. [b] Supercell with 6 formula units.

The nuclei and core electrons are represented with ultrasoft pseudo-potentials, and all structures are fully relaxed with respect to internal and external cell parameters. The wave functions are expanded in plane waves with kinetic energy below 400 eV, and Brillouin zone integration is performed with a 6 × 6 × 4 and 6 × 3 × 4 mesh in the supercells with respectively three and six formula units. Absolute energies were converged with respect to *k*-point sampling. All calculations were performed with spin polarization, previously demonstrated to be crucial in manganese oxides.[15] Both ferromagnetically and anti-ferromagnetically (antiparallel) spin polarized was taken into account in the charge density. Partial states of lithiation were investigated at $x = {}^2/_3$ and $^1/_3$ in a supercell with three formula units and at $x = {}^5/_6$, $^2/_3$, $^1/_2$, $^1/_3$, and $^1/_6$ in a supercell with six formula units. There are respectively three and six distinct Li sites in the supercell with three and six formula units. Therefore, the number of possible Li arrangements is 1, 3, 3, and 1 corresponding to $x = 1$, $^2/_3$, $^1/_3$, and 0. The number of possible Li arrangements would be 1, 6, 15, 20, 15, 6, and 1 for $x = 1$, $^5/_6$, $^2/_3$, $^1/_2$, $^1/_3$, $^1/_6$, and 0, respectively. All the possible arrangements, for the supercell with three formula units have been calculated but only part of the possible arrangements in the supercell with six formula units have been calculated.

Experimental Section

$LiNi_{1/3}Co_{1/3}Mn_{1/3}O_2$ powders were synthesized by a sol−gel method using citric acid as a chelating agent.[16,17] A stoichiometric amount of lithium acetate ($Li(CH_3COO)\cdot 2H_2O$), nickel acetate ($Ni(CH_3COO)_2\cdot 4H_2O$), cobalt nitrate ($Co(NO_3)_2\cdot 6H_2O$), and manganese acetate ($Mn(CH_3COO)_2\cdot 4H_2O$) was dissolved in distilled water and mixed with aqueous solution of citric acid. The resulting solution was mixed with a magnetic stirrer at 80−90 °C for 5−6 h to obtain a clear viscous gel. The gel was dried in a vacuum oven at 140 °C for 24 h. The $LiNi_{1/3}Co_{1/3}Mn_{1/3}O_2$ compound was ground and calcined at 800 and 900 °C after precalcining the obtained precursor at 450 °C. During heating and cooling, the variation of the temperature was fixed as 2 °C/min.

Li, Co, Ni, and Mn contents in the resulting materials were analyzed using an inductively coupled plasma/atomic emission spectrometer (ICP/AES, Kontron S-35). Electrochemical characterization was carried out with coin-type cells. The cathode was prepared by mixing an 85:3.5:1.5:10 (w/w) ratio of active material, carbon black, KS-6 graphite, and polyvinylidene fluoride binder, respectively, in *N*-methyl pyrrolidinone. The resulting paste was applied on an aluminum current collector. The entire assembly was dried under vacuum overnight and then heated in an oven at 120 °C for 2 h. Lithium metal (FMC Corporation) was used as an anode and a polypropylene separator was used to separate anode and the cathode; 1.0 M $LiPF_6$ dissolved in a 1:1 mixture of ethylene carbonate (EC)/diethyl carbonate (DEC) was used as an electrolyte. The cells were assembled in an argon-filled glovebox where both moisture and oxygen content were <1 ppm. The charge and discharge cycles were carried out at a 0.3 C-rate over a potential range between 3.0 and 4.5 V.

X-ray absorption spectroscopy (XAS) experiments were carried out in transmission mode at beam line BL-17C at the National Synchrotron Radiation Research Center (NSRRC) in Hsinchu, Taiwan. The storage ring was operated with an electron energy of 1.5 GeV and a current between 100 and 200 mA. A Si(111) double-crystal monochromator was employed for energy selection. High-order harmonic contamination was rejected by mirrors. The intensities of the incident and transmitted beams were measured by gas ionization chambers. Energy scans of the sample were performed at Ni, Co, and Mn K-edges and the references of Ni, Co, and Mn foils, respectively, were measured simultaneously.

Results and Discussion

(A) Computational. *(1) Structural Parameters of $Li_xNi_{1/3}Co_{1/3}Mn_{1/3}O_2$.* Table 1 shows the calculated lattice parameters of $Li_xNi_{1/3}Co_{1/3}Mn_{1/3}O_2$ at various lithium contents. At each Li composition, the data are given for the Li arrangement with the lowest energy, though we found no significant difference in the structural parameters among various configurations at the same composition. It was found that the lattice parameter a decreases with a decrease in x in the range of $^1/_2 \le x \le 1$ but remains almost unchanged in the range of $^1/_3 \le x \le {}^1/_2$ and then increases with a decrease in x in the range of $0 \le x \le {}^1/_3$. In contrast, the lattice parameter c increases with a decrease in x in the range of $^1/_2 \le x \le 1$ but changes insignificantly in the range of $^1/_3 \le x \le {}^1/_2$ and then decreases again with a decrease in x in the range of $0 \le x \le {}^1/_3$. The bond distances between the transition metal ions and oxygen ions at different lithium contents are also shown in Table 1. The bond distances of Ni−O, Co−O, and Mn−O in a fully lithiated compound ($x = 1$) are (4 × 2.05 Å; 2 × 2.07 Å), (4 × 1.95 Å; 2 × 1.96 Å), and (6 × 1.94 Å), respectively. There is no local Jahn−Teller distortion found in the fully lithiated $LiNi_{1/3}Co_{1/3}Mn_{1/3}O_2$, implying the absence of Jahn−Teller active Ni^{3+} or Mn^{3+}. The large Ni−O bond distance and the absence of a Jahn−Teller distortion indicate a +2 oxidation state for Ni. The bond distances of Co−O (2 × 1.89 Å; 4 × 1.94 Å) and Mn−O (2 × 1.90 Å, 2 × 1.93 Å, 2 × 1.94 Å) decrease only slightly in going to the partially delithiated compound $Li_{2/3}Ni_{1/3}Co_{1/3}Mn_{1/3}O_2$ while those of Ni−O (2 × 1.88 Å; 4 × 2.04 Å) change drastically. The Ni^{3+} octahedron in $Li_{2/3}Ni_{1/3}Co_{1/3}Mn_{1/3}O_2$ has a negative Jahn−Teller distortion. While in pure Ni^{3+} compounds such as $LiNiO_2$ the Jahn−Teller distortion is positive, a negative Jahn−Teller distortion in $Li_{2/3}Ni_{1/3}Co_{1/3}Mn_{1/3}O_2$ is likely induced by the compressive effect of the Co and Mn on

(16) Hwang, B. J.; Santhanam, R.; Liu, D. G.; Tsai, Y. W. *J. Power Sources* **2001**, *102*, 326.
(17) Hwang, B. J.; Santhanam, R.; Liu, D. G. *J. Power Sources* **2001**, *101*, 8612.

the Ni−O bond length. Since a negative Jahn−Teller distortion has a small negative volume effect, it may be the stable distortion when the Ni^{3+} is compressed.[18] At the delithiated compound of $Li_{1/3}Ni_{1/3}Co_{1/3}Mn_{1/3}O_2$, the bond distances of Ni−O, Co−O, and Mn−O are (4 × 1.91 Å; 2 × 1.93 Å), (4 × 1.90 Å; 2 × 1.93 Å), and (2 × 1.91 Å, 2 × 1.92 Å, 2 × 1.93 Å), respectively. We show in one of the next sections that at this composition Ni is oxidized to Ni^{4+}. All of the bond distances decrease slightly more at the fully delithiated compound of $Ni_{1/3}Co_{1/3}Mn_{1/3}O_2$.

(2) Formation Energy of $Li_xNi_{1/3}Co_{1/3}Mn_{1/3}O_2$. In general alloy theory[19] a measure of the effective Ni−Co−Mn interactions can be obtained by comparing the energy of $LiNi_{1/3}Co_{1/3}Mn_{1/3}O_2$ to the average energy of $LiNiO_2$, $LiCoO_2$, and $LiMnO_2$, that is, $\Delta E_{mix} = E(LiNi_{1/3}Co_{1/3}Mn_{1/3}O_2) - {}^1/_3[E(LiNiO_2) + E(LiCoO_2) + E(LiMnO_2)]$. If ΔE_{mix} is negative, Ni, Co, and Mn have on average an attractive interaction and the system will be either randomly mixed or ordered, depending on the strength of the interaction and the preparation temperature. If ΔE_{mix} is positive, local phase separation into Ni-, Co-, or Mn-rich regions is energetically favorable, though random mixing may be achieved if the synthesis temperature is high enough. From calculating the relevant energy values in the above formula, it was found that ΔE_{mix} for $LiNi_{1/3}Co_{1/3}Mn_{1/3}O_2$ is −105 meV per formula unit, indicating an attractive tendency among Ni, Co, and Mn. It also implies that the synthesis of this material is thermodynamically favorable. Similarly, for the fully delithiated material $\Delta E_{mix} = E(Ni_{1/3}Co_{1/3}Mn_{1/3}O_2) - {}^1/_3[E(NiO_2) + E(CoO_2) + E(MnO_2)]$ is computed to be 44 meV, indicating repulsive Ni−Co−Mn interactions. The interactions go from being attractive in $LiNi_{1/3}Co_{1/3}Mn_{1/3}O_2$ to being repulsive in $Ni_{1/3}Co_{1/3}Mn_{1/3}O_2$. Hence, to remove lithium, one has to supply not only the binding energy for the lithium ion and electron but also the strong energy increase in the system due to the Ni−Co−Mn interactions on the transition-metal layer becoming unfavorable.

The definition of relative formation energy (E_{RF}) for a given Li-vacancy arrangement with concentration x in $Li_xNi_{1/3}Co_{1/3}Mn_{1/3}O_2$ is given as[20]

$$\Delta E_{RF} = E(Li_xNi_{1/3}Co_{1/3}Mn_{1/3}O_2) - (x)E(LiNi_{1/3}Co_{1/3}Mn_{1/3}O_2) - (1-x)E(Ni_{1/3}Co_{1/3}Mn_{1/3}O_2)$$

where $E(\,)$ is the total energy of the configuration per $Li_xNi_{1/3}Co_{1/3}Mn_{1/3}O_2$ formula unit. These relative formation energies are convenient for displaying the possible stability of intermediate states with Li-vacancy ordering. The relative formation energies for $Li_xNi_{1/3}Co_{1/3}Mn_{1/3}O_2$, as shown in Figure 1, are negative, indicating the stability of intermediate compounds or solid solutions, depending on temperature.

(3) Density of States of $Li_xNi_{1/3}Co_{1/3}Mn_{1/3}O_2$. To analyze the changes in the electronic structure with lithium deintercalation, the density of states at different Li concentrations is shown in Figure 2. The density of states is presented here for the configuration with lowest total energy. In the lowest energy arrangement Co and Mn were anti-ferromagnetic at $x = 0$. At $x = {}^2/_3$ and $x = 1$ anti-ferromagnetic Ni and Mn had the lowest energy. Since the transition-metal ions occupy the octahedral sites in the sublattice of oxygen, the 3d bands of the transition-metal ions are split into the t_{2g} and e_g bands. In $LiNi_{1/3}Co_{1/3}Mn_{1/3}O_2$, the up-spin Ni t_{2g}, Co t_{2g}, and Ni e_g bands and down-spin Ni t_{2g}, Co t_{2g}, and Mn t_{2g} bands are fully occupied, corresponding to Ni $t_{2g}^6e_g^2$, Co t_{2g}^6, and Mn t_{2g}^3. The highest occupied (lowest unoccupied) states are mainly of Ni e_g (Mn t_{2g}) character. Meanwhile, the filled Co-t_{2g} states overlap with the Ni e_g in energy. Since holes in the Co t_{2g} easily transfer by overlapping of the t_{2g} states through the common edge of the MO_6 octahedra, the mobility of electrons or holes in this material can be similar to that in $LiCoO_2$.

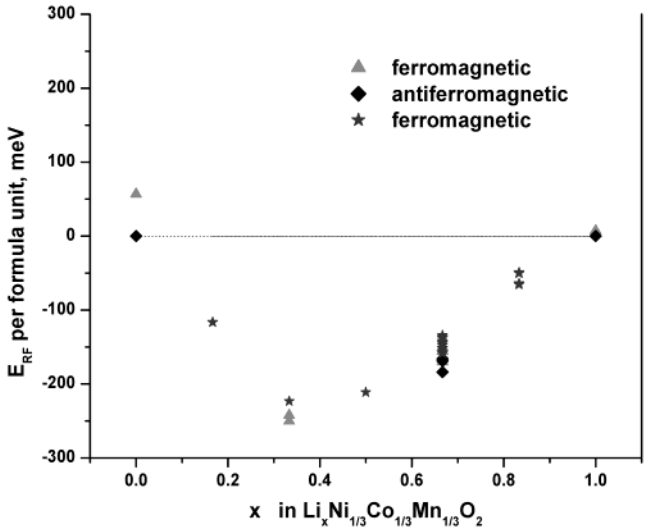

Figure 1. Relative formation energy (E_{RF}) of $Li_xNi_{1/3}Co_{1/3}Mn_{1/3}O_2$. ▲, calculation with ferromagnetic coupling in a supercell of 3 formula units; ♦, calculation with antiferromagnetic coupling in a supercell of 3 formula units; ★, calculation with ferromagnetic coupling in a supercell of 6 formula units.

In the case of $Li_{2/3}Ni_{1/3}Co_{1/3}Mn_{1/3}O_2$, an electron is removed from the Ni e_g band with an up-spin state (Figure 2b), indicating that the redox reaction of Ni^{2+}/Ni^{3+} takes place in the range of ${}^2/_3 \le x \le 1$. To evaluate whether Ni^{3+} disproportionates into Ni^{2+} and Ni^{4+}, 15 Li arrangements in a 6 formula-units supercell of $Li_{2/3}Ni_{1/3}Co_{1/3}Mn_{1/3}O_2$ were calculated. No charge disproportionation of Ni^{3+} was observed. The Fermi energy level is located in the Ni e_g band. The band gap between the highest occupied bands and the lowest unoccupied bands becomes much smaller than that of $LiNi_{1/3}Co_{1/3}Mn_{1/3}O_2$, implying that the conductivity of the delithiated compound in the range of ${}^2/_3 \le x \le 1$ might be better than the fully lithiated compounds.

When more Li is extracted to form $Li_{1/3}Ni_{1/3}Co_{1/3}Mn_{1/3}O_2$, an electron is further removed from the Ni e_g band as shown in Figure 2c. It indicates that the redox reaction of Ni^{3+}/Ni^{4+} takes place in the range of ${}^1/_3 \le x \le {}^2/_3$. The O 2p band shifts further to higher energy and causes stronger interaction between

(18) Marianetti, C. A.; Morgan, D.; Ceder, G. *Phys. Rev. B* **2001**, *63* (22), 4304.
(19) de Fontaine, D. In *Solid State Physics*; Ehrenreich, H., Turnbull, D., Eds.; Academic Press: New York, 1994; Vol. 47, p 33.
(20) Van der Ven, A.; Aydinol, M. K.; Ceder, G.; Kresse, G.; Hafner, J. *Phys. Rev. B* **1998**, *58* (6), 2975.

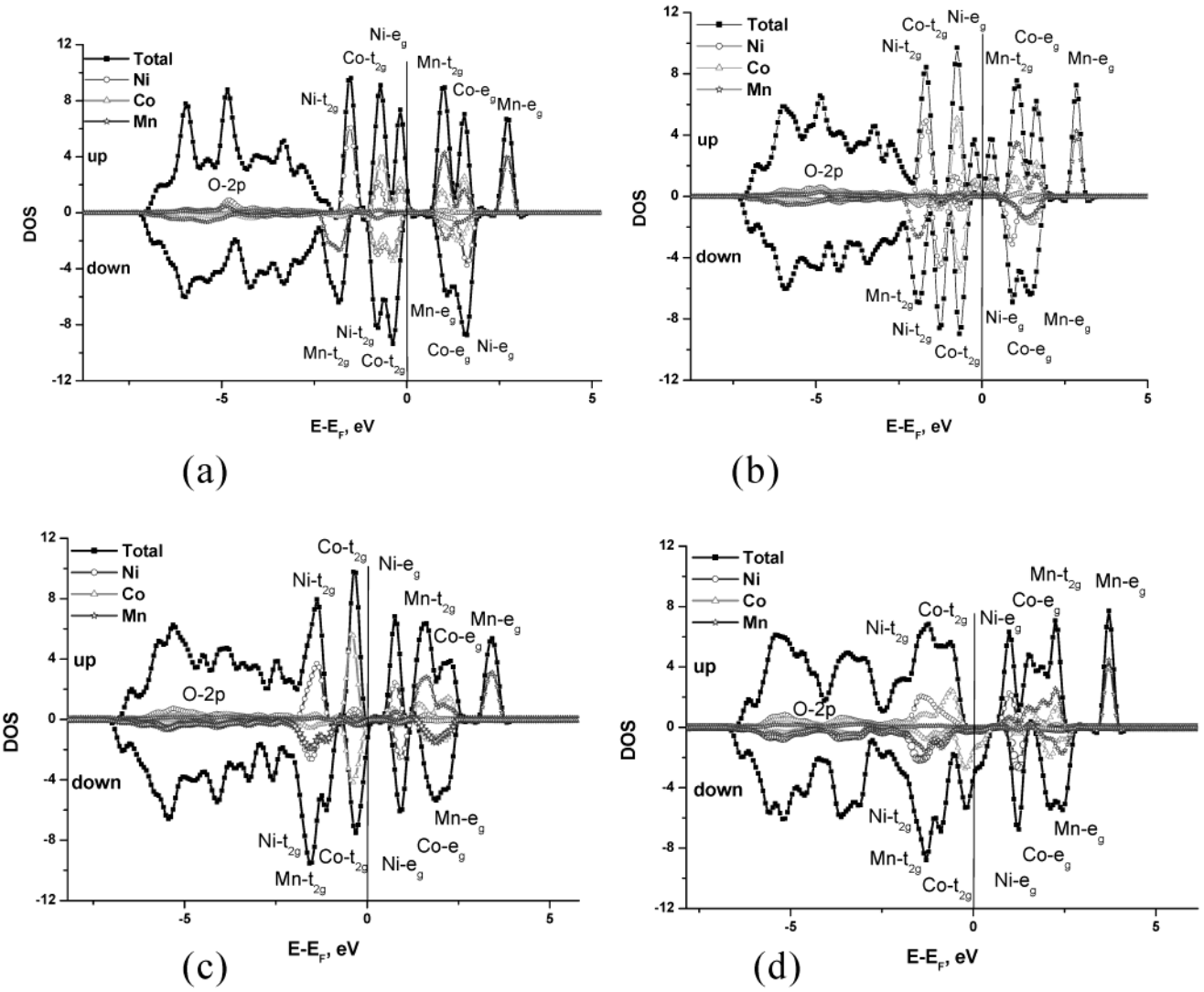

Figure 2. Density of states of $Li_xNi_{1/3}Co_{1/3}Mn_{1/3}O_2$ at (a) $x = 1$, (b) $x = {}^2/_3$, (c) $x = {}^1/_3$, and (d) $x = 0$.

O 2p orbitals and t_{2g} bands of transition metals. This will lead to a stronger hybridization of the metal−oxygen orbitals, resulting in more covalency of the remaining electrons as Li is extracted. Upon further extraction of Li to $Ni_{1/3}Co_{1/3}Mn_{1/3}O_2$, an electron is removed from the Co t_{2g} band as shown in Figure 2d, indicating that Co^{3+} is oxidized to Co^{4+} in the range of $0 \leq x \leq {}^1/_3$.

(4) Charge and Spin States. The valence state of a high-spin transition-metal ion can be determined by integrating the spin-polarization density in a sphere around the ion. Integrating spin density is much more effective than integrating the charge density, as the former filters out the electronic contribution from the O 2p bands, which usually carry very little net electron spin. For the relevant ions, Ni^{2+}, Ni^{3+}, and Ni^{4+}, we expect a total electron spin count of respectively ± 2, ± 1, and 0 (in units of 1/2 μ_B). For Co^{3+} and Co^{4+} we expect 0 and ± 1, respectively. For Mn^{2+}, Mn^{3+}, and Mn^{4+} we expect ± 5, ± 4, and ± 3, respectively. The integrated spin density for $Li_xNi_{1/3}Co_{1/3}Mn_{1/3}O_2$ for various values of x is shown in Figure 3. In $LiNi_{1/3}Co_{1/3}Mn_{1/3}O_2$ (Figure 3a) the integrated moment of Ni increases steeply as we integrate through the d-states of the Ni ion, but then reaches a plateau value because the charge density of the oxygen ions does not contribute to the spin density. After this plateau the integrated value decreases as spin from the neighboring Mn ions is picked out (which is antiparallel to the Ni^{2+} moment). The moment around Ni is slightly below what is expected for Ni^{2+}. The remainder of the moment is probably on the oxygen ions, as is typical for nickel oxides.[21] It indicates that the oxidation state of the Ni ion in $LiNi_{1/3}Co_{1/3}Mn_{1/3}O_2$ is +2. In contrast, the integrated moment of Mn decreases steeply as we integrate through the d-states of the Mn ion, but then reaches a plateau value. After this plateau the integrated value increases due to the contribution of spin from the neighboring Ni ions. It reveals that the oxidation state of the Mn ion in $LiNi_{1/3}Co_{1/3}Mn_{1/3}O_2$ is +4. The lack of moment on Co indicates an oxidation state of +3. These results further confirm that the formal valence states are $LiNi_{1/3}{}^{II}Co_{1/3}{}^{III}Mn_{1/3}{}^{IV}O_2$. In the case of $Li_{2/3}Ni_{1/3}Co_{1/3}Mn_{1/3}O_2$, only the net moment of Ni is changed and becomes 1, as shown in Figure 3b, indicating that the formal valence states are $Li_{2/3}Ni_{1/3}{}^{III}Co_{1/3}{}^{III}Mn_{1/3}{}^{IV}O_2$. When one lithium ion is

(21) Reed, J.; Ceder, G. *Electrochem. Solid-State Lett.* **2002**, *5* (7), A145.

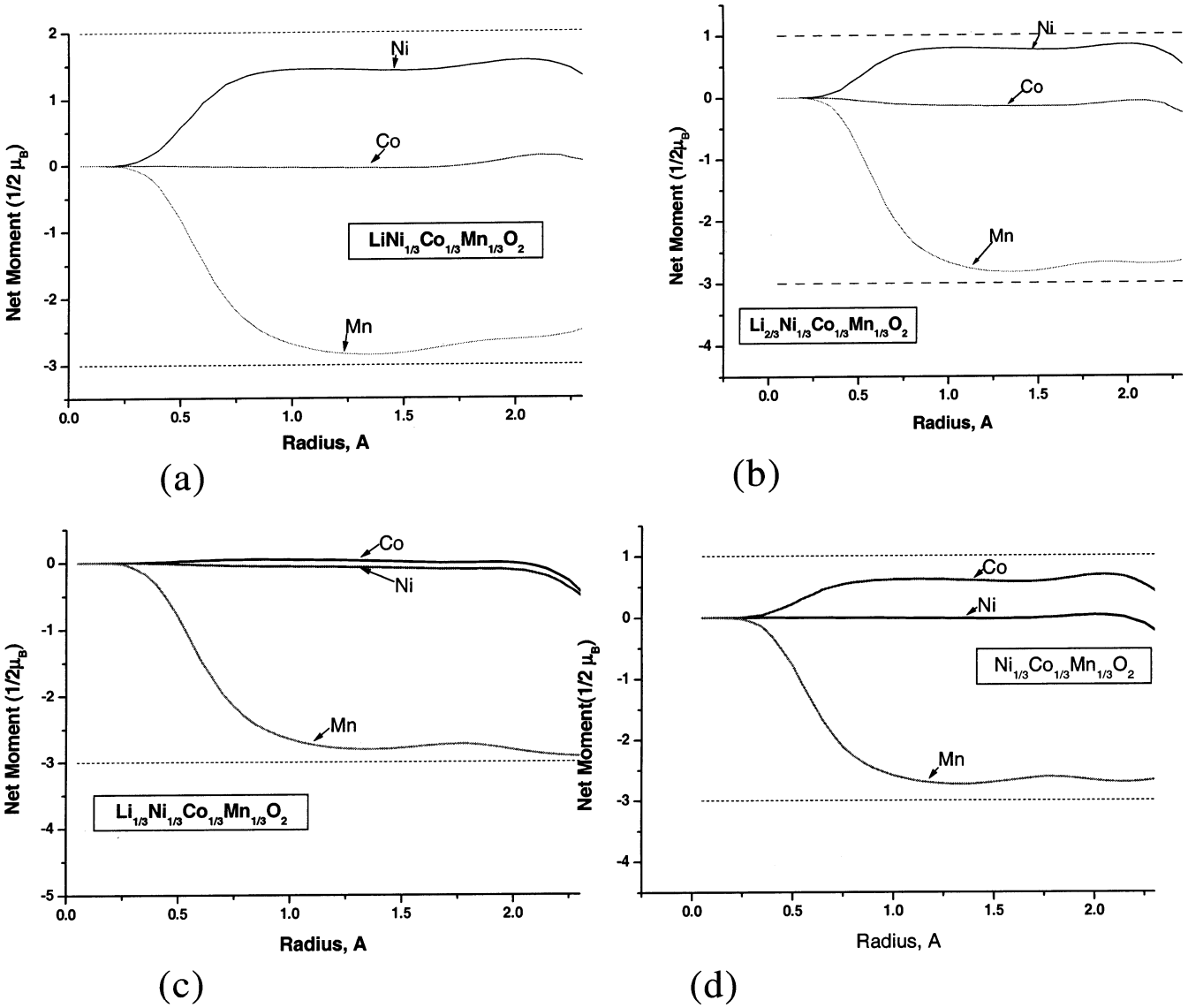

Figure 3. Integrated spin as a function of integration radius (Å) around Ni, Co, and Mn in $Li_xNi_{1/3}Co_{1/3}Mn_{1/3}O_2$ at (a) $x = 1$, (b) $x = {}^2/_3$, (c) $x = {}^1/_3$, and (d) $x = 0$.

extracted further, only the net moment of Ni is changed again and becomes zero in $Li_{1/3}Ni_{1/3}Co_{1/3}Mn_{1/3}O_2$, implying formal valence states of $Li_{1/3}Ni_{1/3}{}^{IV}Co_{1/3}{}^{III}Mn_{1/3}{}^{IV}O_2$. Extracting the last Li ion in the supercell only modifies the net moment of Co, indicating that it is becoming oxidized to Co^{4+}.

(5) Calculated Voltage Curve as a Function of Li Content. The open circuit voltage curve can be calculated with well-established methods,[20,22] though it is rather computationally intensive. A reasonable approximation to the voltage curve can be obtained by calculating the average voltage over parts of the Li composition domain. The average voltage for $LiNi_{1/3}Co_{1/3}Mn_{1/3}O_2$ in the range of $a \le x \le b$ is given as

$$V = \{E(\mathrm{Li}_a\mathrm{Ni}_{1/3}\mathrm{Co}_{1/3}\mathrm{Mn}_{1/3}\mathrm{O}_2) - E(\mathrm{Li}_b\mathrm{Ni}_{1/3}\mathrm{Co}_{1/3}\mathrm{Mn}_{1/3}\mathrm{O}_2) + (b-a)E(\mathrm{Li})\}/(b-a)\mathrm{e}$$

The result is given in Figure 4. One should keep in mind that these voltages are typically underpredicted. The voltage is a gently sloping curve in the range $1/3 < x < 1$. For $0 < x < {}^1/_3$, the calculated average voltage is high as the redox reaction of Co^{3+}/Co^{4+}occurs. This high potential may be a significant impediment for extracting all the Li from this material.

(B) Experimental. *(1) Synthesis of $LiNi_{1/3}Co_{1/3}Mn_{1/3}O_2$.* The structure of the $LiNi_{1/3}Co_{1/3}Ni_{1/3}O_2$ powders synthesized by sintering at 900 °C for 12 h was characterized using X-ray diffraction (XRD)(Cu Kα radiation), as shown in Figure 5. This figure reveals that the prepared sample has the typical layered structure of α-$NaFeO_2$ type with space group $R\bar{3}m$. No impurity-related peaks have been observed from the XRD pattern of $LiNi_{1/3}Co_{1/3}Ni_{1/3}O_2$. The two small peaks between 20 and 25° in 2θ are coming from Vaseline added to the sample. The clear splitting of the lines assigned to the Miller indices (006, 102) and (108, 110) in Figure 5 indicates good characteristics of the layered structure. It implies that this material with an α-$NaFeO_2$ structure can be successfully synthesized by the sol−gel method. This is consistent with the prediction from the negative formation energy shown in the computational prediction. A partial interchange of occupancy of Li and transition-metal ions would give rise

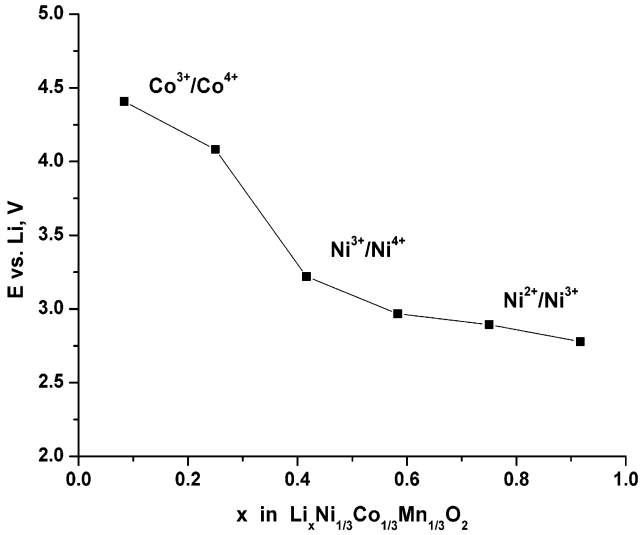

Figure 4. Calculated average voltage points in $Li_xNi_{1/3}Co_{1/3}Mn_{1/3}O_2$ for intervals $^n/_6 < x < {}^{(n+1)}/_6$ (n = 1, 2, 3, 4, and 5).

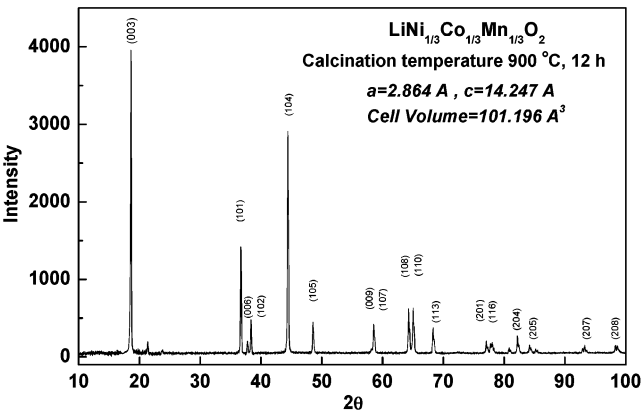

Figure 5. XRD pattern of the synthesized $Li_xNi_{1/3}Co_{1/3}Mn_{1/3}O_2$ powders sintered at 900 °C for 12 h.

to cation mixing (disordering) in the structure. The R value, the integrated intensity ratio of the (003) to (104) lines, is used to measure the degree of cation mixing. The smaller the R value, the higher the disordering. If R is <1.2, it means that undesirable cation mixing takes place.[23] The R value of 1.36, indicating no undesirable cation mixing, is observed in this sample. Shaju et al. have reported an R value of 0.8 in their samples synthesized by a mixed hydroxide method. It means that the poor capacity retention of their samples might result from the undesirable cation mixing. The lattice parameters a and c were determined to be 2.864 and 14.247 Å, respectively. These data match well with the values observed by Ohzuku and Makimura (a = 2.867 Å and c = 14.246 Å) and Shaju et al. (a = 2.864 Å and c = 14.233 Å). The calculated values are slightly larger than those measured, as is often the case for computations in the generalized gradient approximation.

(2) XANES of $LiNi_{1/3}Co_{1/3}Mn_{1/3}O_2$. X-ray absorption near-edge structure (XANES) provides information about the valence state of the absorbing atom. The

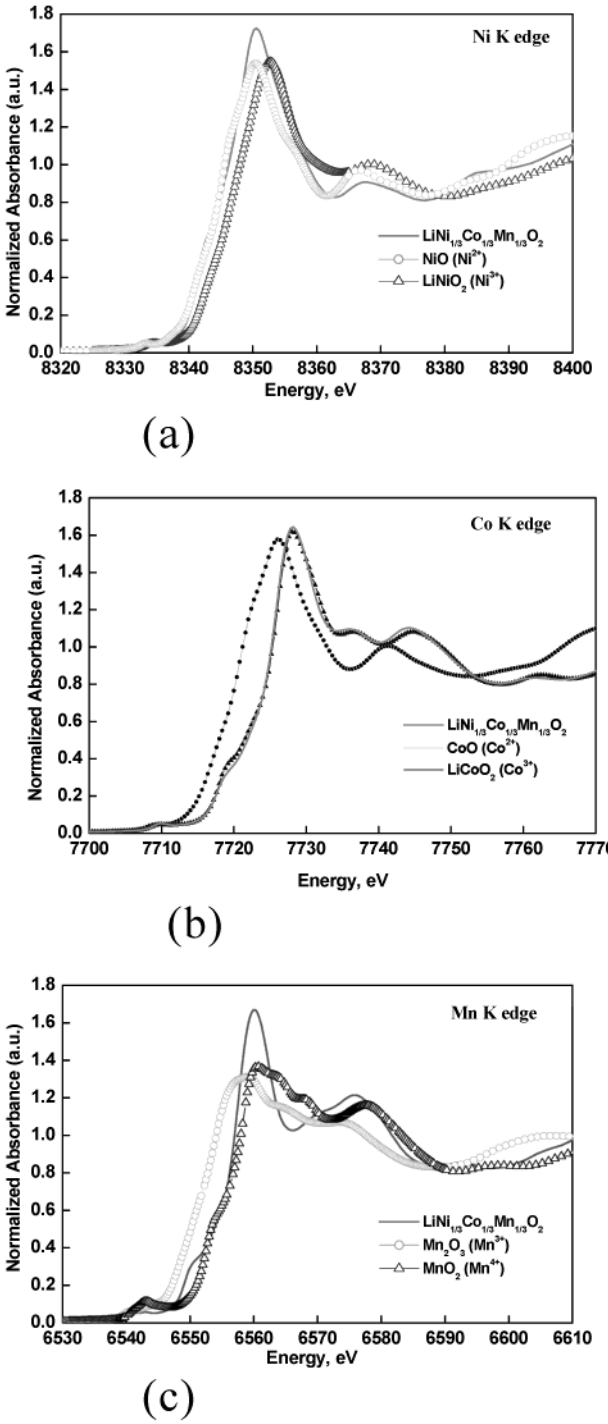

Figure 6. Normalized XANES spectra for $LiNi_{1/3}Co_{1/3}Mn_{1/3}O_2$ at (a) Ni K-edge compared with the spectra of NiO and $LiNiO_2$. (b) Co K-edge compared with the spectra of CoO and $LiCoO_2$. (c) Mn K edge compared with the spectra of MnO_2 and Mn_2O_3.

XANES results obtained for the $LiNi_{1/3}Co_{1/3}Mn_{1/3}O_2$ material are shown in this work. Parts (a), (b), and (c) of Figure 6 show the Ni, Co, and Mn K-edges XANES spectra of this material, respectively. The XANES spectra of reference materials for Ni^{2+}(NiO), Ni^{3+}($LiNiO_2$), Co^{2+}(CoO), Co^{3+}($LiCoO_2$), Mn^{3+}(Mn_2O_3), and Mn^{4+}(MnO_2) are also given in Figure 6 for comparison. As can be easily observed in Figure 6a−c, the Ni, Co, and Mn edges of the $LiNi_{1/3}Co_{1/3}Mn_{1/3}O_2$ material almost coincide with the edges of NiO, $LiCoO_2$, and MnO_2. It indicated that the valence states of Ni, Co, and

(22) Aydinol, M. K.; Kohan, A. F.; Ceder, G.; Cho, K.; Joannopoulos, J. *Phys. Rev. B* **1997**, *56*, 1354.
(23) Ohzuku, T.; Ueda, A.; Nagayama, M.; Iwakoshi, Y.; Komori, H. *Electrochim. Acta* **1993**, *38*, 1159.

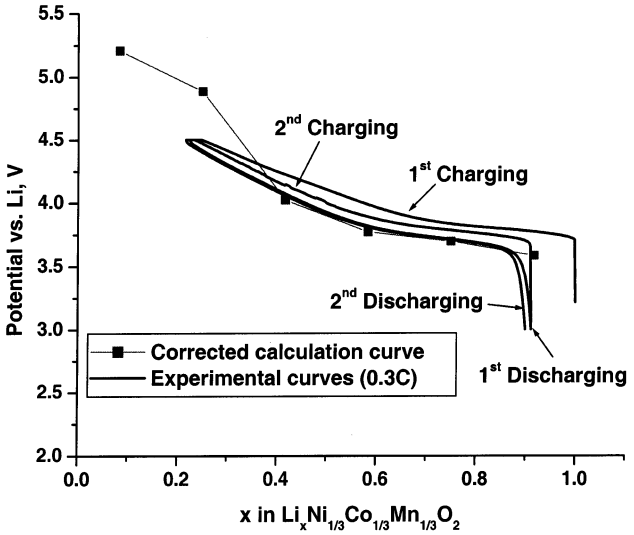

Figure 7. First and second charge/discharge curves of $LiNi_{1/3}Co_{1/3}Mn_{1/3}O_2$ materials sintered at 900 °C for 12 h in the voltage range of 3.0−4.5 V at 0.3 C.

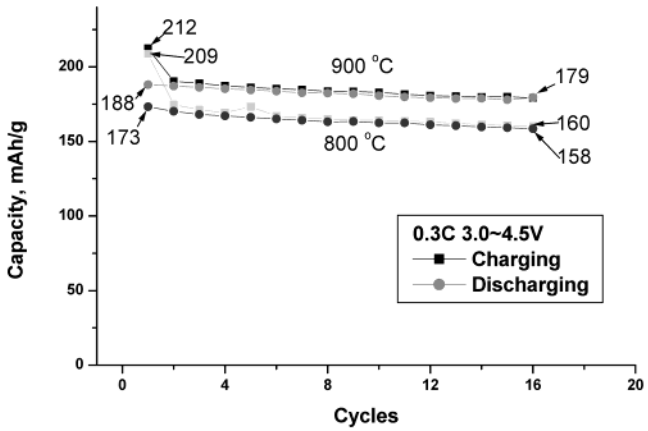

Figure 8. Charge and discharge capacity vs cycle number curves of the $LiNi_{1/3}Co_{1/3}Mn_{1/3}O_2$ materials sintered at 800 and 900 °C for 12 h.

Mn in $LiNi_{1/3}Co_{1/3}Mn_{1/3}O_2$ are +2, +3, and +4, respectively, in good agreement with the calculated valence states.

(3) Charge−Discharge Curve and Cyclability. The first and second charge and discharge curves of a $Li/LiNi_{1/3}Co_{1/3}Mn_{1/3}O_2$ cell, in the voltage range of 3.0−4.5 V and at a constant current rate of 0.3 C, are given in Figure 7. The electrolyte uses 1.0 M $LiPF_6$ dissolved in a 1:1 mixture of ethylene carbonate (EC)/diethyl carbonate (DEC). There is one plateau around 3.8 V in the range of $^1/_3 \le x \le 1$ in $Li_xNi_{1/3}Co_{1/3}Mn_{1/3}O_2$. The experimental potentials are higher than the calculated values, as is typical with standard first-principles energy methods.[22] The potential difference between the calculated and experimental data is suggested to be 0.7−0.8 V.[21] The correction of 0.8 V was added to the calculated potential to give the result which can be compared directly with the experimental values, as shown in Figure 7. It was found that the tendency of the experimental charge−discharge curves is consistent with that of the calculated one in the range of $^1/_3 \le x \le 1$. The calculated average potentials after correction in the range of $^1/_6 \le x \le ^1/_3$ and $0 \le x \le ^1/_6$ in $Li_xNi_{1/3}Co_{1/3}Mn_{1/3}O_2$ are 4.88 and 5.20 V, respectively. Since most of the electrolytes will be decomposed at a potential higher than 5.0 V, it indicates that at least $^1/_6$ of the lithium may be difficult to extract from this material. Therefore, the practical specific capacity of this material will likely be <228 mA h/g. The cyclability of the $LiNi_{1/3}Co_{1/3}Mn_{1/3}O_2$ material synthesized at 800 and 900 °C is shown in Figure 8. Both data points demonstrate good cyclability. The first charge and discharge capacities for the material synthesized at 900 °C were 212 and 188 mA h/g, respectively. The first charge and discharge capacities for the material synthesized at 800 °C were 209 and 173 mA h/g, respectively. The irreversible capacities of the $LiNi_{1/3}Co_{1/3}Mn_{1/3}O_2$ material synthesized at 800 and 900 °C can be determined to be 36 and 24 mA h/g, respectively. The irreversible capacity is due to the part of Ni that cannot be reduced during the discharging process at this C-rate from the in situ X-ray absorption spectroscopy (XAS) observation of $LiNi_{1/3}Co_{1/3}Mn_{1/3}O_2$ during charging/discharging processes. A systematic study of this will be presented in a forthcoming paper. The cell performance of the $LiNi_{1/3}Co_{1/3}Mn_{1/3}O_2$ material synthesized at 900 °C is shown to be better than that of the $LiNi_{1/3}Co_{1/3}Mn_{1/3}O_2$ material synthesized at 800 °C. It may result from a higher degree of crystallinity obtained at higher temperature.

Conclusion

The paper presents a combined first-principles/experimental study of $LiNi_{1/3}Co_{1/3}Mn_{1/3}O_2$. The material was successfully synthesized by a sol−gel process and shows good initial specific capacity and cyclability at a 0.3 C-rate in the range of 3.0−4.5 V. The oxidation states of Ni, Co, and Mn in the starting material of $LiNi_{1/3}Co_{1/3}Mn_{1/3}O_2$ are demonstrated to be +2, +3, and +4, respectively, from both the calculated and XANES data. As a result, the couples are Ni^{2+}/Ni^{3+} and Ni^{3+}/Ni^{4+} if the lithium content (x) is in the range of $^2/_3 \le x \le 1$ and $^1/_3 \le x \le ^2/_3$, respectively. In the range of $0 \le x \le ^1/_3$, the redox reaction is Co^{3+}/Co^{4+}. The latter causes a significant increase of voltage near the end of charge and may be an impediment to obtaining more capacity from this material. Our results indicate that $LiNi_{1/3}Co_{1/3}Mn_{1/3}O_2$ material is a high-capacity electrode and has excellent capacity retention for advanced rechargeable lithium ion batteries. The irreversible capacity of $Li_xNi_{1/3}Co_{1/3}Mn_{1/3}O_2$ probably has to be reduced before it can be commercialized.

Acknowledgment. The support from the Education Ministry (EX-91-E-FA09-5-4), National Synchrotron Radiation Research Center (NSRRC), and National Taiwan University of Science and Technology of Taiwan is gratefully acknowledged. This work was also supported in part by the MRSEC Program of the National Science Foundation under award number DMR 02-13282.

CM030299V